

OPEN ACCESS

EDITED BY

Reza Taherdangkoo, Freiberg University of Mining and Technology, Germany

REVIEWED BY

Ebrahim Sharifi Teshnizi, Ferdowsi University of Mashhad, Iran Umar Zada, Polytechnic Institute of New York University, United States

*CORRESPONDENCE

Wenwei Li,

■ 180804010002@hhu.edu.cn

RECEIVED 22 September 2025 REVISED 15 October 2025 ACCEPTED 15 October 2025 PUBLISHED 10 November 2025

CITATION

Qiu X, Lai Z, Zuo J and Li W (2025) Synergistic stabilization of expansive soil using ultrafine high-reactivity fly ash and calcium carbide slag: performance optimization and microstructural insights.

Front. Mater. 12:1710809.
doi: 10.3389/fmats.2025.1710809

COPYRIGHT

© 2025 Qiu, Lai, Zuo and Li. This is an open-access article distributed under the terms of the Creative Commons Attribution License (CC BY). The use, distribution or reproduction in other forums is permitted, provided the original author(s) and the copyright owner(s) are credited and that the original publication in this journal is cited, in accordance with accepted academic practice. No use, distribution or reproduction is permitted which does not comply with these terms.

Synergistic stabilization of expansive soil using ultrafine high-reactivity fly ash and calcium carbide slag: performance optimization and microstructural insights

Xingwang Qiu¹, Zhenrui Lai¹, Jinyu Zuo² and Wenwei Li^{3,4}*

¹PowerChina Chengdu Engineering Corporation Limited, Chengdu, China, ²Laboratory of Ministry of Education for Geomechanics and Embankment Engineering, Hohai University, Nanjing, China, ³Postdoctoral Research Station, Shandong University, Jinan, China, ⁴Postdoctoral Workstation, Jiangsu Hanjian Group Co., Ltd., Yangzhou, China

Expansive soils pose significant geotechnical challenges to infrastructure due to their moisture-induced shrink-swell behavior. Traditional stabilizers often have environmental or cost drawbacks. This study investigates a sustainable stabilization technique using a synergistic binder system composed of ultrafine high-reactivity fly ash (UHFA) and calcium carbide slag (CCS), two industrial by-products. The primary contribution of this research is the systematic optimization of both the binder ratio and total dosage to maximize engineering performance. A comprehensive laboratory program, including compaction, free swelling rate, and unconfined compressive strength (UCS) tests, was conducted, supplemented by scanning electron microscopy (SEM) and X-ray Diffraction (XRD) for microstructural analysis. Results indicate that an optimal UHFA:CCS mass ratio of 7:3 and a total binder content of 15% yields the best performance. Under these optimal conditions, the 28-day free swelling rate was reduced to 27.4%, effectively reclassifying the soil as non-expansive, while the UCS reached a peak of 378.1 kPa, approximately 4.5 times that of the untreated soil. Mechanistically, SEM and XRD analyses revealed that CCS provides an alkaline environment that activates the pozzolanic reactivity of UHFA, generating extensive C-S-H and C-A-H gels. These gels fill pores and bind soil particles into a dense, stable skeleton, while Ca2+ ion exchange further mitigates swelling potential. This study demonstrates that the optimized UHFA-CCS system is a high-performance, resource-efficient technology for mitigating expansive soil issues.

KEYWORDS

expansive soil, soil stabilization, ultrafine high-reactivity fly ash, calcium carbideslag, unconfined compressive strength (UCS)

1 Introduction

Expansive soils, typically rich in hydrophilic smectite minerals such as montmorillonite, are characterized by significant moisture-induced volumetric changes (shrink-swell) (Zada et al., 2023; Barman and Dash, 2022; Jalal et al., 2021). These properties, along

with other environmental factors such as thermal variations (Zhang et al., 2026) and the long-term, time-dependent creep behavior of geotechnical materials that can affect the stability of soil structures (Tong et al., 2025a; Liu and Shu, 2025; Tong et al., 2025b), present severe challenges to engineering practice and are widely encountered in many regions of China (Ikeag et al., 2019; Yao et al., 2024). In large-scale infrastructure projects such as mining, water conservancy, and transportation, expansive soil foundations have long been recognized as a major geotechnical concern (Puppala, 2021; Biswas et al., 2024). In drainage systems, tailings dams, and ore transport roads, the cyclic swelling and shrinkage of expansive soils often result in slope instability, subgrade settlement, and cracking of embankments, thereby threatening both structural safety and economic performance (Dang et al., 2021; Zimar et al., 2022; Dai et al., 2024). Consequently, a range of ground improvement techniques, from chemical stabilization to the use of mechanical reinforcements like steel fibers in concrete structures, are employed to mitigate these risks in challenging geotechnical environments (Sun et al., 2025; Ezazi et al., 2024; Sharifi Teshnizi et al., 2024).

To suppress the shrink-swell behavior and enhance service stability, stabilization using additives has been widely adopted. Traditional stabilizers such as lime and cement have a long history of use in improving the properties of problematic soils, including collapsing and expansive soils (Hashemi et al., 2023; Lv et al., 2025). However, the production of these traditional binders has a significant environmental footprint, prompting a shift towards more sustainable alternatives derived from industrial by-products (Almuaythir et al., 2024). This trend towards sustainability is prevalent across the civil engineering discipline, from developing novel soil binders to creating high-performance structural composites with alternative resources like seawater and sea-sand (Fu et al., 2025). The long-term durability of these alternative binders, especially under aggressive environmental conditions like acid or thermal attack, is a critical area of ongoing research (Teshnizi et al., 2023). Materials such as cement kiln dust (CKD) have been successfully used to improve the geomechanical properties of loess soils, primarily through the formation of cementitious hydration products (Sharifi Teshnizi et al., 2022). Among these by-products,fly ash and calcium carbide slag are commonly employed, and their combined use has been shown to improve soil structure, strength, and durability (Almuaythir et al., 2024). With the advancement of green mining concepts, the in situ utilization of industrial waste generated within mining areas has emerged as a sustainable trend.

Fly ash, produced in large quantities from coal-fired power plants (Karami et al., 2021; Abdila et al., 2022), is regarded as a potential soil stabilizer that can reduce swelling potential and improve bearing capacity (American Coal Ash Association, 2003; White et al., 2005). Similarly, calcium carbide slag (CCS), also known as calcium carbide residue (CCR), is a highly alkaline by-product of acetylene production rich in calcium hydroxide [Ca(OH)₂]. The synergistic use of CCR and fly ash as a cementitious material for soil stabilization has been previously established. Horpibulsuk, Phetchuay and Chinkulkijniwat (Horpibulsuk et al., 2012) demonstrated that this combination effectively improves the strength of silty clay, with the Ca(OH)₂ in CCR providing the alkaline environment necessary to activate the pozzolanic fly ash, leading to the formation of cementitious products. Nevertheless,

the modification efficiency of ordinary fly ash is often constrained by the heterogeneity of particle size distribution and variability in pozzolanic reactivity, which may limit early-age strength development (Snellings et al., 2021).

The concept of combining an alkaline activator with a silica- and alumina-rich source extends to the field of geopolymer technology and the use of nano-materials. For instance, Li et al. (Li et al., 2021)successfully used CCR as part of a combined activator system for coal gangue (another silica-alumina waste) to create a geopolymer binder feasible for soil stabilization, highlighting the role of CCR in promoting the formation of N-A-S-H and C-A-S-H gels. In parallel, recent studies have shown that nanomaterials, such as nano-silica, can be combined with activators like lime or cement to significantly enhance soil properties. The inclusion of nano-silica can improve the strength and durability of marl soils (Mirzababaei et al., 2021) and can help mitigate adverse reactions, such as ettringite formation, in sulfate-bearing soils by promoting the development of C-S-H gel (Karimiazar et al., 2023). This approach often allows for a reduction in the required amount of traditional binders like cement while achieving superior performance (Karimiazar et al., 2022). These studies underscore a common principle: pairing a calcium-based activator with a highly reactive pozzolanic material can create a highly effective and sustainable binder system.

Drawing from this principle, ultrafine high-reactivity fly ash (UHFA) presents a promising alternative to conventional fly ash for use with CCS (Cai et al., 2024). Its smaller particle size, larger specific surface area, and higher content of reactive oxides promote rapid dissolution of amorphous silica and alumina, thereby accelerating the generation of calcium silicate hydrate (C-S-H) and calcium aluminate hydrate (C-A-H) gels (Zhang et al., 2021; Wang and Dong, 2023). These hydrates fill voids and enhance microstructural densification, improving both early- and long-term strength (Akmalaiuly et al., 2023). While the foundational work of Horpibulsuk, Phetchuay and Chinkulkijniwat (Horpibulsuk et al., 2012) confirmed the viability of the CCR-FA system, a systematic investigation focused on the enhanced performance offered by ultrafine high-reactivity fly ash has not been thoroughly conducted. Specifically, there is a need to optimize the mixture proportions and total dosage of the UHFA-CCS system for expansive soils and to quantify the benefits through a detailed analysis of mechanical performance, microstructural evolution, and economic efficiency.

Despite promising results from previous studies combining CCS with traditional fly ash, a systematic investigation into the use of ultrafine high-reactivity fly ash remains a key research gap. The enhanced reactivity of UHFA suggests the potential for superior performance but requires careful optimization of mix proportions and dosages to be effective and economical. Therefore, the primary innovation of this research is the comprehensive optimization of a UHFA-CCS binder system and the detailed characterization of its performance-mechanism relationship. The objective of this research is to establish a cost-effective and environmentally sustainable stabilization technique for expansive soils by systematically investigating the synergistic mechanisms of ultrafine high-reactivity fly ash and calcium carbide slag. Compaction tests, free swell measurements, unconfined compressive strength tests at different curing ages, and microstructural analyses are conducted to evaluate the effects of mix ratio and dosage. The findings provide both







Expansive soil (ES)

Ultrafine high-reactivity Calcium carbide slag (CCS) fly ash(UHFA)

FIGURE 1

The experimental material used in this test.

TABLE 1 Basic properties of expansive soil used.

| Index | Liquid limit $w_{\rm L}$ (%) | Plastic limit w _P (%) | Plasticity index I _P (%) | Specific gravity $G_{ m s}$ |
|-------|------------------------------|----------------------------------|-------------------------------------|-----------------------------|
| Value | 51.2 | 23.6 | 27.6 | 2.72 |

theoretical understanding and practical guidance for engineering construction in expansive soil regions, while simultaneously promoting the resource utilization of industrial by-products. The proposed method is anticipated to have wide application in mine dump slope stabilization, tailings dam reinforcement, goaf backfilling, and other geotechnical projects, supporting solid-waste recycling and the advancement of green construction.

2 Materials and methods

2.1 Materials

This study employed the expansive soil (as shown in Figure 1) collected from Gaochun District, Nanjing, Jiangsu Province, at a depth of 2–3 m below ground level. This depth was chosen to bypass the upper topsoil and weathered layers, ensuring a homogeneous sample representative of the parent expansive clay formation. The bulk sample was air-dried under laboratory conditions, passed through a 2 mm sieve, and then characterized for basic index properties. The liquid limit, plastic limit, plasticity index, and specific gravity were 51.2%, 23.6%, 27.6%, and 2.72, respectively (Table 1), and the particle-size distribution curves are provided in the original manuscript (Figure 1).

A ultrafine high-reactivity fly ash (as shown in Figure 1) produced by mechanical ultrafine grinding served as the principal reactive aluminosilicate. It is characterized by a mean particle size $<\!10\,\mu m$, a high specific surface area, and enhanced pozzolanic reactivity; the oxide composition is summarized in Table 2. Calcium carbide slag (as shown in Figure 1), an alkaline by-product of acetylene production dominated by portlandite [Ca(OH) $_2\approx93$ wt%], was sourced from a chemical plant in Hunan Province. Gradation curves for UHFA and CCS are reported alongside that of the soil in Figure 2 of the original manuscript, and both binders met routine quality requirements for soil stabilization.

2.2 Experiment methods

A two-stage program decoupled the influence of binder proportion from total dosage. In Stage I, the total binder content (UHFA + CCS) was fixed at 20% of dry soil, while the UHFA:CCS mass ratio λ was varied to identify an optimal proportion ($\lambda_{\rm opt}$). In Stage II, the proportion was fixed at λ opt and the total binder dosage $w_{\rm UHFA-CCS}$ was set to 5%, 10%, 15%, 20%, and 25% of dry soil. The range of binder ratios (5:5 to 9:1) and total dosages (5%–25%) was selected based on a review of relevant literature on soil stabilization and the results of preliminary laboratory trials to ensure the optimal formulation would be captured within the experimental design.

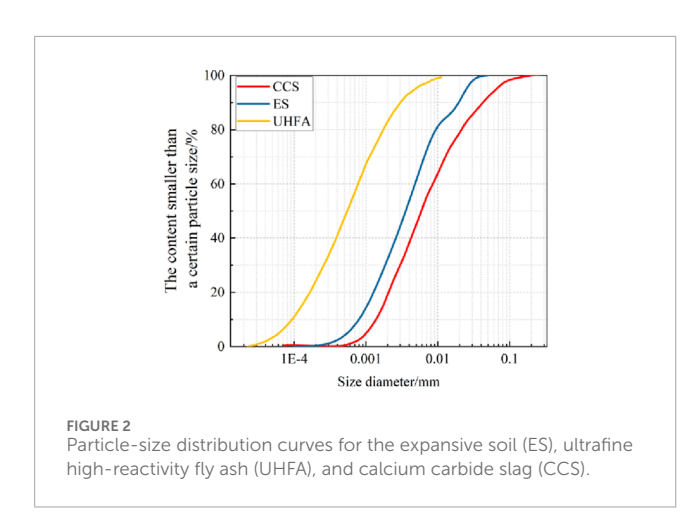
The overall process of the experimental procedure is shown in Figure 3. As shown in Figure 3a, to ensure homogeneity, the airdried and ground soil and binders were first mixed in a dry state for 5 minutes, after which water was added and the mixture was blended for another 5 minutes. For potential field applications, methods such as *in situ* mixing with a rotary tiller or *ex-situ* plant mixing could be considered. As shown in Table 3, All prepared specimens for UCS and microstructural tests were carefully sealed in plastic wrap to prevent moisture loss and cured in a standard humidity chamber at a constant temperature of 20 °C \pm 2 °C and a relative humidity exceeding 95% for the specified periods (7, 14, or 28 days).

The experimental program was conducted in general accordance with the procedures outlined in the Chinese Standard for Geotechnical Testing Method (GB/T 50123-2019) (Ministry of Construction P.R.China, 2019). The primary laboratory tests included the light compaction test, the free swelling rate test, the unconfined compressive strength (UCS) test, scanning electron microscopy (SEM) and X-ray diffraction (XRD) analysis. The specific procedures for each test are detailed below.

Light Proctor compaction test (as shown in Figure 3b) was performed to determine the maximum dry density (MDD) and optimum moisture content (OMC) of the untreated and

TABLE 2 Index properties of the expansive soil.

| Component | SiO ₂ | Al ₂ O ₃ | Fe ₂ O ₃ | CaO | SO ₃ | Others |
|-----------|------------------|--------------------------------|--------------------------------|-----|-----------------|--------|
| Content/% | 65.4 | 21.3 | 4.5 | 6.2 | 2.2 | 0.4 |



stabilized soil mixtures. Sieved soil samples, prepared at a series of predetermined moisture contents, were compacted in a standard mold in three equal layers. Each layer was subjected to a specified number of blows from a standard rammer with a controlled drop height to ensure a consistent compactive effort. After compaction, the bulk density and moisture content of each specimen were determined. The dry density was then calculated, and the results were used to plot a compaction curve (dry density *versus* moisture content), from which the MDD and OMC were obtained. These parameters are crucial for evaluating the soil's compactability and guiding field compaction control.

The free swelling rate, an index used to characterize the swell potential of the soil, was determined using the graduated cylinder method (as shown in Figure 3c). For each test, a 10 g sample of ovendried and sieved expansive soil was gently placed into a 100 mL graduated cylinder, and its initial volume was recorded. The cylinder was then slowly filled with deionized water, allowing the sample to fully inundate and swell freely under no external confinement. After the volume of the soil ceased to increase (typically after 24 h), the final swollen volume was recorded. The free swelling rate (FSR) was calculated as the percentage increase in volume relative to the initial volume.

The unconfined compressive strength (UCS) test (as shown in Figure 3d) was conducted to evaluate the strength and stiffness of the cured soil specimens. Cylindrical specimens were prepared at their respective MDD and OMC using static compaction in three equal layers to ensure uniform density throughout the sample. They were then sealed and cured for specified periods (7, 14, and 28 days). Each cured specimen was then placed in a uniaxial compression apparatus and subjected to a constant axial strain rate (e.g., 1%/min) until failure occurred or a peak stress was reached (Chen et al., 2025). The UCS was calculated as the maximum axial stress (the peak load divided by the initial cross-sectional area) that the specimen

could sustain. This parameter is a key indicator of the effectiveness of the stabilization treatment and the engineering applicability of the improved soil.

To investigate the stabilization mechanisms at the microlevel, both scanning electron microscopy (SEM) and X-ray diffraction (XRD) analyses were performed. For SEM analysis (as shown in Figure 3e), small, representative fragments were carefully extracted from the interior of fractured UCS specimens, freeze-dried to preserve their internal structure, and then sputter-coated with a thin layer of gold for observation with a high-resolution SEM. This provided direct visual evidence of the soil fabric, particle arrangement, and the morphology of cementitious hydration products. Complementing this, XRD analysis (as shown in Figure 3f) was conducted to identify the mineralogical composition. For XRD, samples were oven-dried at 60 °C, ground into a fine powder passing a No. 200 sieve (75 μ m), and analyzed using a diffractometer with Cu Ka radiation over a 2θ range from 10° to 80°. Together, the XRD diffractograms offered definitive mineralogical proof of the formation of new products such as portlandite, calcium silicate hydrates (C-S-H), and calcium aluminate hydrates (C-A-H), while the SEM micrographs revealed how these new products were physically distributed to create a denser, cemented soil skeleton.

3 Results and analysis

3.1 Optimal UHFA:CCS proportion at a fixed total dosage

The initial experimental phase identified the A3 mixture, formulated with a 7:3 ratio of UHFA to CCS at a 20% total binder content, as the optimal proportion due to its superior comprehensive performance in compaction, free swell, and unconfined compressive strength tests. As depicted in Figure 4, the compaction test results show that while the maximum dry density (MDD) for the A3 mixture decreased slightly to 1.53 g/cm³ compared to the 1.60 g/cm³ of the untreated control soil (A0), its optimal moisture content (OMC) increased from 17.0% to 18.6%. This trend is consistent across all specimens, where a higher UHFA proportion systematically led to a lower MDD and a higher OMC. This phenomenon is attributed to two primary mechanisms: the reduction in MDD is caused by the replacement of denser soil particles with lower specific gravity UHFA and the immediate flocculation of clay particles induced by the CCS, while the increase in OMC is a direct consequence of the water consumed during the pozzolanic hydration reactions and the higher water adsorption demand from the large specific surface area of the ultra-fine fly ash. Therefore, the selection of the A3 ratio as optimal is based on achieving a balance that maximizes the generation of cementitious

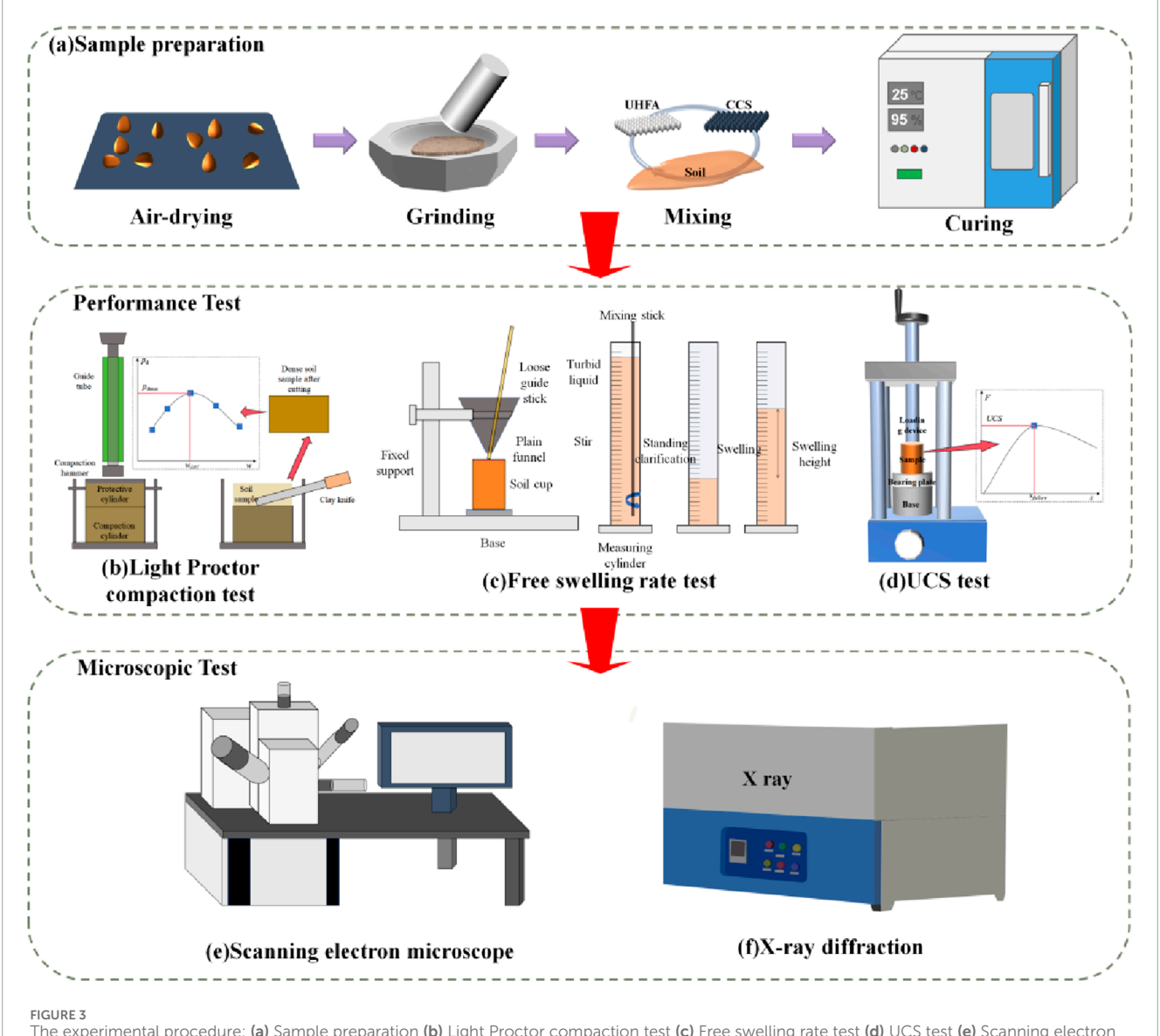


FIGURE 3
The experimental procedure: (a) Sample preparation (b) Light Proctor compaction test (c) Free swelling rate test (d) UCS test (e) Scanning electron microscope (f) X-ray diffraction.

products for long-term performance enhancement, rather than solely on achieving the highest density or the fastest early-age strength gain.

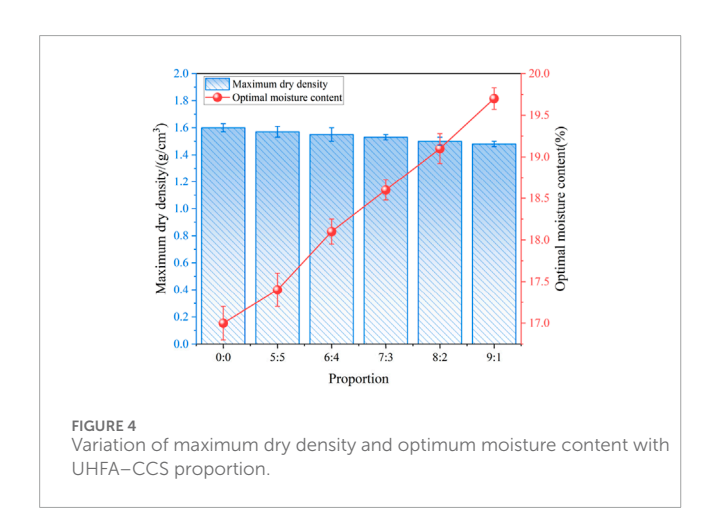
As depicted in Figure 5, the 7-day free swelling rate tests demonstrate the profound efficacy of the ultrafine high-reactivity fly ash and calcium carbide slag binder in mitigating the swell potential of the expansive soil. The optimal A3 mixture (UHFA:CCS = 7:3) reduced the swell ratio from 68.1% in the untreated soil to 29.8%, a significant improvement that reclassifies the material as non-expansive by falling below the common 30% engineering threshold. This result is part of a consistent trend where swell suppression was enhanced with increasing UHFA content, reaching a minimum of 24.6% for the A5 (9:1) specimen. This powerful synergistic effect is attributable to a multi-faceted mechanism. Initially, calcium ions (Ca²⁺) from the CCS induce immediate cation exchange and flocculation of clay particles, creating a more

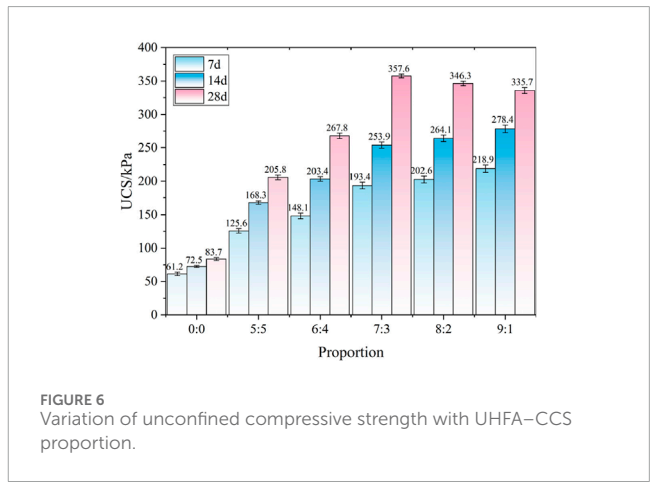
stable soil fabric with a lower affinity for water. Concurrently, the high-pH environment activates the pozzolanic UHFA, forming time-dependent cementitious products (C-S-H and C-A-H) that crystallize within the soil pores. These hydrates provide a robust physical restraint that mechanically prevents particle swelling and refines the pore structure, thereby impeding further water ingress.

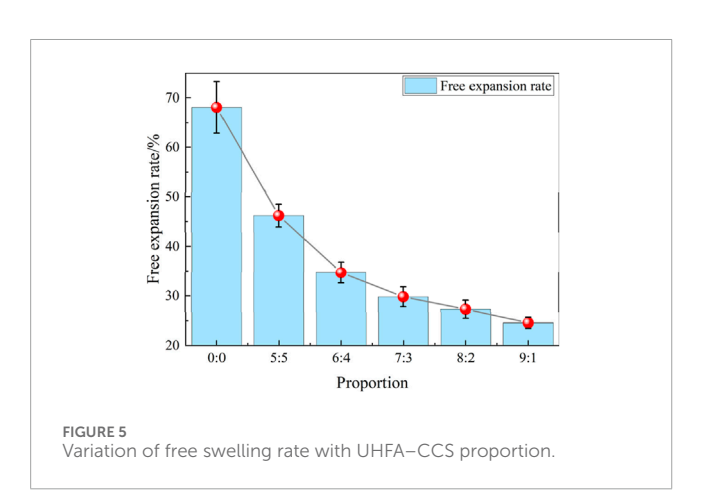
Regarding the unconfined compressive strength (UCS), the results presented in Figure 6 indicate that the A3 specimen (UHFA:CCS = 7:3) achieved values of 193.4 kPa, 253.9 kPa, and 357.6 kPa at 7, 14, and 28 days, respectively. These values are substantially higher than those of the untreated control group (61.2 kPa, 72.5 kPa, and 83.7 kPa) and demonstrate a superior overall performance compared to the other stabilized mixtures. It is noteworthy that while the A4 (8:2) and A5 (9:1) mixtures yielded competitive, or even higher, strengths at early curing ages (7 and 14 days), their final 28-day strengths were ultimately lower than that

TABLE 3 Summary of the experimental program, mix designs, and tests conducted.

| Experimental stage | Group | UHFA (% of dry soil) | CCS (% of dry soil) | UHFA:CCS (λ) | Total binder (w _{UHFA-CCS} /%) | Curing ages (v/d) |
|-----------------------|-------|-------------------------|---------------------------------------|--|--|----------------------|
| | A0 | 0 | 0 | 0 | 0 | |
| | A1 | 10 | 10 | 5:5 | 20 | |
| | A2 | 12 | 8 | 6:4 | 20 | |
| 1 | A3 | 14 | 6 | 7:3 | 20 | |
| | A4 | 16 | 4 | 8:2 | 20 | |
| | A5 | 18 | 2 | 9:1 | 20 | 7, 14, 28 |
| | B1 | 5×λ _{optUHFA} | 5×λ _{optCCS} | | 5 | |
| | B2 | 10×λ _{optUHFA} | $10 \times \lambda_{\mathrm{optCCS}}$ | | 10 | |
| 2 | В3 | 15×λ _{optUHFA} | 15×λ _{optCCS} | $\lambda_{optUHFA}$: λ_{optCCS} | 15 | |
| | A3\B4 | 20×λ _{optUHFA} | $20 \times \lambda_{optCCS}$ | | 20 | |
| | B5 | 25×λ _{optUHFA} | $25 \times \lambda_{\text{optCCS}}$ | | 25 | |

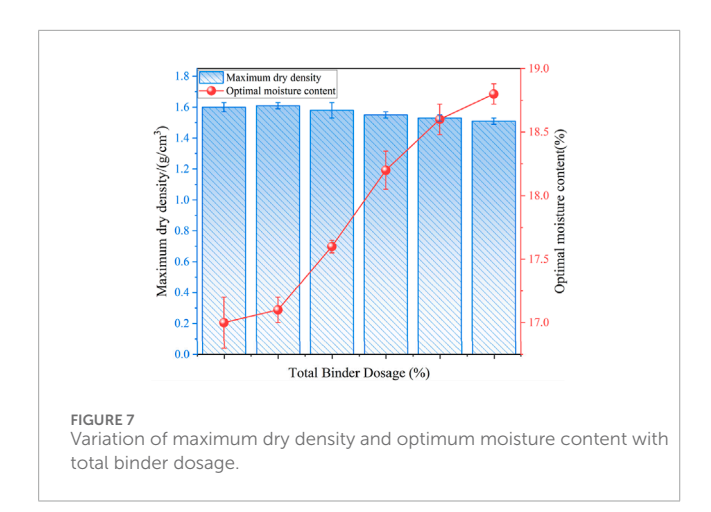






of the A3 specimen. This time-dependent behavior suggests that a higher proportion of reactive UHFA can accelerate initial pozzolanic reactions and early strength gain. However, for long-term strength development, the reduced quantity of the CCS activator in these mixtures appears insufficient to facilitate the complete and sustained reaction of the abundant fly ash, leading to a less durable and less efficiently cemented soil matrix over time. The 7:3 ratio in the A3 mixture appears to provide a more balanced supply of reactants, promoting a steadier and more complete hydration process that culminates in superior 28-day strength, a critical parameter for the design of engineering structures.

Consequently, the A3 mixture, with a UHFA:CCS ratio of 7:3, is identified as the optimal mix proportion from this phase of the study, as it not only effectively suppresses swelling but also demonstrates a distinct advantage in achieving both a favorable dry density and superior long-term strength gain. Based



on this comprehensive analysis, the A3 mix exhibits the most outstanding performance in meeting the two critical objectives of swell suppression and bearing capacity enhancement. To further investigate the mechanisms and synergistic effects of UHFA and CCS at varying dosages, the subsequent research phase will utilize this optimal ratio (UHFA:CCS = 7:3). This next stage will examine the soil's compaction, strength, and deformation characteristics under different total binder contents of 5%, 10%, 15%, 20%, and 25%, aiming to provide more refined technical guidance for practical engineering design by evaluating the influence of binder quantity on both modification efficiency and project cost.

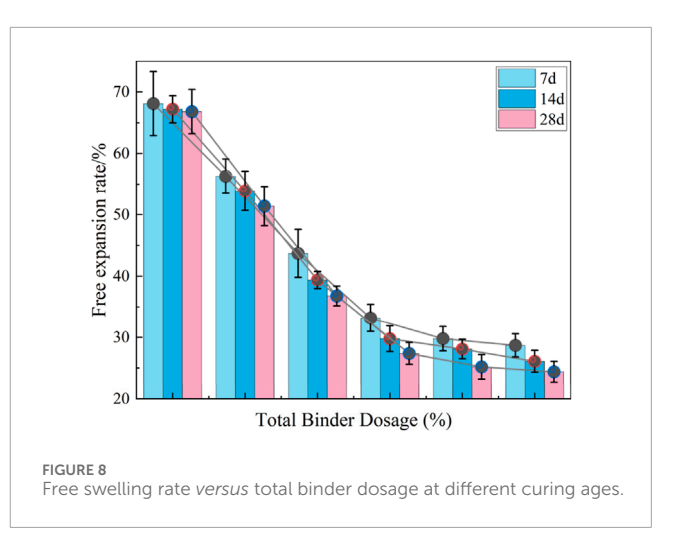
3.2 Optimal total binder dosage at a fixed proportion

3.2.1 Compaction behavior

The compaction test results for the second experimental phase, presented in Figure 7, reveal a systematic trend as the total dosage of the optimal 7:3 UHFA-CCS binder was increased from 5% to 25%. While the effect was minimal at a low 5% dosage, at higher contents the maximum dry density (MDD) progressively decreased from 1.61 g/cm³ to 1.51 g/cm³, while the optimal moisture content (OMC) correspondingly increased from 17.1% to 18.8%. This behavior is governed by the progressive replacement of dense soil particles with the lighter binder and the enhanced flocculation of the soil fabric, which lowers MDD. Concurrently, the rise in OMC is a direct consequence of the increased water demand for the pozzolanic reactions that form voluminous Calcium-Silicate-Hydrate (C-S-H) gels. From a practical engineering perspective, a binder content in the 15%-20% range represents an optimal balance, providing significant improvements in mechanical properties without the diminishing returns and higher material costs associated with larger dosages, thus offering a performance-optimized and cost-effective solution for field applications.

3.2.2 Free swelling rate

As illustrated in Figure 8, the Free swelling rate of the stabilized soil exhibits a significant, progressive reduction with both increasing total binder content (from 5% to 25%) and extended curing time. The specimen with a 5% dosage (B1) showed limited swell

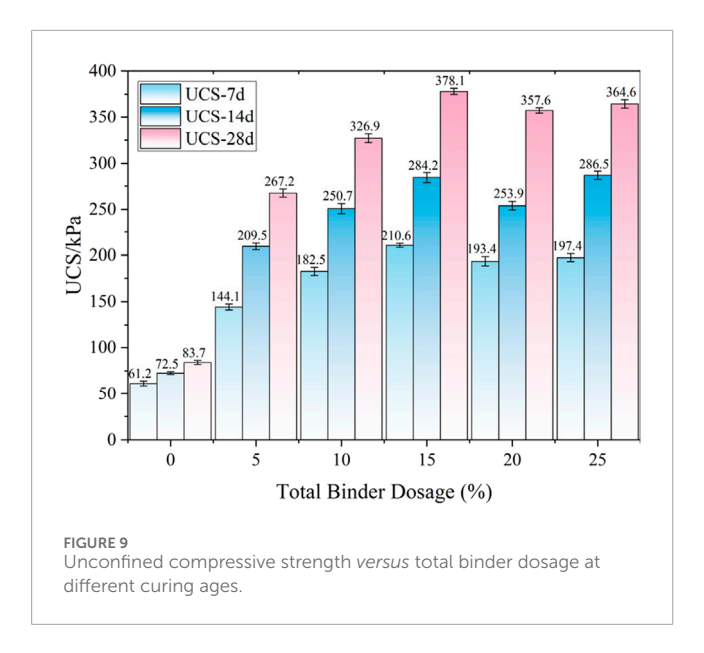


mitigation, with its 28-day Free swelling rate remaining high at 51.4%. Increasing the dosage to 10% (B2) provided a more noticeable improvement, reducing the 28-day value to 36.8%, yet still falling within the expansive soil category. A critical threshold was crossed with the 15% dosage (B3), where the Free swelling rate decreased to 29.8% at 14 days and 27.4% at 28 days, effectively transitioning the soil to a non-expansive state according to the common 30% engineering criterion. The 20% (B4/A3) and 25% (B5) dosages further enhanced this effect, achieving non-expansive states within the first 7 days of curing and reaching final 28-day Free swelling rates of 25.2% and 24.4%, respectively. While the 25% dosage yielded the lowest Free swelling rate, the marginal improvement over the 20% dosage was minimal.

This time-dependent behavior demonstrates that increasing the UHFA-CCS binder content accelerates and intensifies the swell suppression mechanisms. At higher dosages, a more extensive and dense network of cementitious products (C-S-H and C-A-H gels) forms rapidly throughout the soil matrix. This network provides a dual function: it physically restrains the clay particles, and it fills and refines the pore structure, thereby obstructing the migratory pathways of water to the expansive mineral surfaces. As curing progresses, these pozzolanic reactions continue, further solidifying the soil fabric and leading to the observed continued decrease in Free swelling rate over time. However, from a practical standpoint, an optimal dosage must balance performance with economic and engineering efficiency. While the 20% and 25% dosages provide the best swell control, the 15% dosage also achieves a nonexpansive state at later curing ages and may be sufficient for many engineering applications. Considering the previous compaction and strength test results, a dosage of 15%-20% is identified as the optimal range, as it effectively reduces swell potential to acceptable levels while maintaining high long-term strength and balancing material costs, thus representing the most pragmatic and cost-effective solution.

3.2.3 Analysis of unconfined compressive strength

The unconfined compressive strength (UCS) development of the stabilized soil as a function of total binder content is presented in Figure 9. The results clearly indicate that while



increasing the binder dosage generally enhances soil strength, this effect is non-linear, with an optimal content beyond which further additions yield diminishing returns. Specifically, the B3 specimen, with a 15% binder dosage, exhibited the highest ultimate strength, reaching 210.6 kPa, 284.2 kPa, and a peak value of 378.1 kPa at 7, 14, and 28 days, respectively. In contrast, the specimens with higher dosages of 20% (A3/B4) and 25% (B5) achieved lower final 28-day strengths of 357.6 kPa and 364.6 kPa. This demonstrates that simply increasing the quantity of the binder does not guarantee a proportional increase in long-term mechanical performance, and that a dosage of 15% represents the most effective formulation for strength development under the tested conditions.

The existence of an optimal dosage can be explained by the efficiency of the pozzolanic reactions and the development of the soil's microstructure. At a 15% dosage, the proportions of the reactive silica and alumina from the UHFA and the alkaline activators from the CCS appear to achieve an ideal stoichiometric balance. This allows for a sustained and efficient hydration process throughout the curing period, resulting in a well-distributed and interconnected network of cementitious products (C-S-H gel) that effectively binds the soil particles and fills the voids. At higher dosages (20% and 25%), however, several factors may limit longterm strength gain. As suggested by the SEM analysis for the 25% dosage specimen (Figure 10c), the excessive amount of binder can lead to localized agglomeration, preventing the homogeneous formation of the stabilizing gel. This non-uniform microstructure can result in "gel blocking," where the surfaces of binder clusters hydrate quickly, forming a low-permeability layer that encapsulates unreacted UHFA and CCS particles in the core. This phenomenon, coupled with a reduction in the effective water-to-binder ratio within these dense agglomerates, hinders the efficient, longterm hydration process and the development of a robust and durable soil skeleton, thus explaining the diminishing returns in strength.

From an engineering and economic perspective, the concept of marginal return is critical in selecting the appropriate binder content. The increase in 28-day strength from a 10% to a 15% dosage is a substantial 51.2 kPa. In contrast, increasing the dosage from 15% to 25% not only requires 10% more material but also results in a net decrease in strength of 13.5 kPa. This clearly indicates that dosages exceeding 15% are not cost-effective and may even be counterproductive to achieving maximum strength. This phenomenon aligns with the general principle in soil stabilization that an optimal binder content exists, beyond which the benefits are outweighed by increased material costs and potential negative impacts on the microstructure. Therefore, considering the balance between mechanical performance, material expenditure, and the associated effects on compaction properties, a 15% total binder content is identified as the optimal and most efficient dosage, providing a technically sound and economically viable solution for the engineering application of this stabilization technique.

3.2.4 Analysis of scanning electron microscope results

Scanning Electron Microscopy (SEM) observations provide a clear visualization of the soil fabric's evolution with increasing binder content, as shown in Figure 10. In the specimen with a low (5%) UHFA-CCS dosage, the stabilization effect is minimal, with only small quantities of flocculent or film-like gels observed adhering to the surfaces of soil particles. As seen in Figure 10a, the inter-particle pore spaces remain large and open, with only sparse and discontinuous cementitious bridges forming locally. A significant transformation occurs as the dosage increases to the optimal level of 15%. Figure 10b reveals a dense, interconnected network of hydration products, such as honeycomb, fibrous, and reticular Calcium-Silicate-Hydrate (C-S-H) gels, forming between the soil particles. These products effectively fill the original voids and create a robust, integrated soil skeleton, which greatly enhances the soil's structural integrity. When the dosage is further increased to 25% (Figure 10c), the cementitious phase becomes even more voluminous in localized areas, but evidence of binder agglomeration and unreacted particles also becomes apparent, disrupting the formation of a uniform skeletal structure.

The observed evolution of the soil's microstructure provides a compelling validation for the macroscopic behavior recorded in the compaction, free swell, and unconfined compressive strength tests. The sparsely distributed gels in the 5% sample correspond to its limited improvement in strength and swell control. In contrast, the dense and well-distributed cementitious matrix of the 15% sample directly explains its superior mechanical performance; the continuous C-S-H network provides a strong binding effect, physically restrains the clay particles against swelling, and refines the pore structure, leading to the highest ultimate strength. The non-uniform microstructure of the 25% sample, with its localized binder agglomerations, elucidates why its long-term strength did not surpass the 15% sample. These dense clumps can limit the efficient hydration of all binder particles and create structural heterogeneity, thus explaining the "diminishing marginal returns" observed in the macroscopic tests. This multi-scale analysis confirms that an optimal binder dosage is crucial for achieving a uniformly cemented and highly stable soil fabric, which is the fundamental basis for effective soil stabilization.

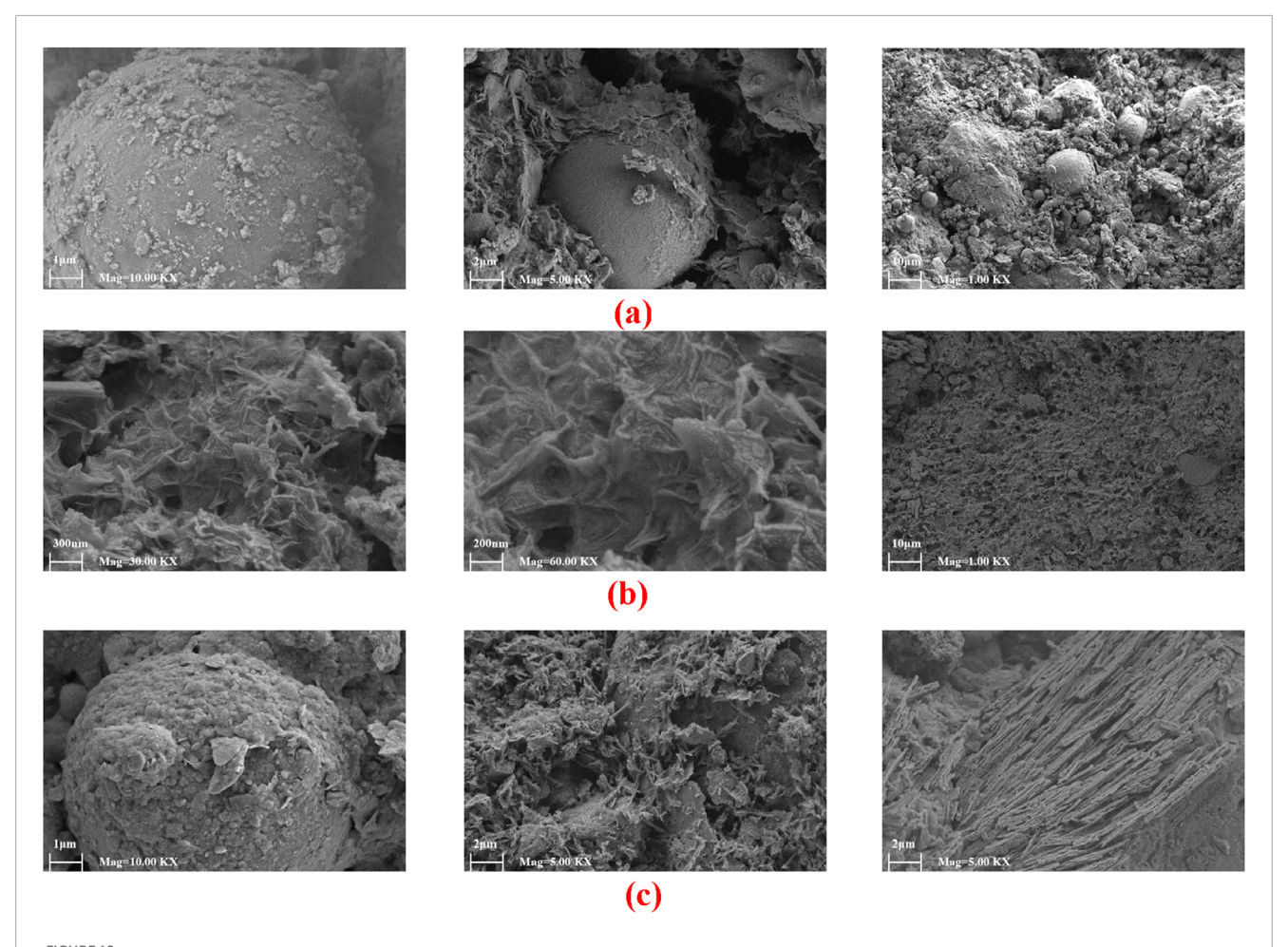


FIGURE 10 Scanning electron microscopy results. (a) Typical microstructure of stabilized soil specimen at a total binder dosage of 5% (b) Typical microstructure of stabilized soil specimen at a total binder dosage of 25%.

3.3 Determination of the optimal UHFA-CCS proportion and binder content

To precisely determine the optimal binder dosage, this study establishes a comprehensive evaluation framework that balances technical performance with economic efficiency and marginal benefits, a goal pursued in materials engineering through both experimental analysis and intelligent computational models (Yu et al., 2025). Three key performance indicators are derived from the 28-day unconfined compressive strength (UCS) data to facilitate this analysis.

First is the Strength Gain (SG(w)) in Equation 1, which quantifies the absolute performance improvement relative to the untreated soil:

$$SG(w) = UCS_w - UCS_0 \tag{1}$$

where UCS_w is the unconfined compressive strength (UCS) at a given binder dosage percentage w, and UCS_0 is the UCS of the untreated soil. is the UCS of the untreated soil (83.7 kPa).

Second is the Performance-Cost Ratio (PCR(w)) in Equation 2, which evaluates the average return on investment. For this analysis, the binder dosage percentage (w) is used as a direct proxy for the

material cost, an assumption that facilitates a technical comparison of efficiency:

$$PCR(w) = \frac{SG(w)}{w} \tag{2}$$

Finally, the Marginal Strength Gain $(MG(w_i))$ in Equation 3 provides the most decisive metric for optimization by revealing the incremental benefit of each additional unit of binder:

$$MG(w_i) = \frac{SG(w_i) - SG(w_{i-1})}{w_i - w_{i-1}}$$
(3)

where w_i and w_{i-1} represent adjacent dosage levels tested in the experiment (e.g., 15% and 10%).

The calculated values for these indicators based on the experimental data are summarized in Table 4.

The evaluation begins with a feasibility screening based on a key engineering criterion: the 28-day free swell index must be below the 30% threshold for non-expansive soil. This defines the technically feasible set, which is the subset of mix designs that meet this essential engineering requirement. In this study, the feasible set includes dosages of 15%, 20%, and 25%. Within this set, the 15% dosage achieves a peak UCS of 378.1 kPa, identifying it as the technically

| TARIF 4 | Indicators | calculated | hased | on the | e experimental data. |
|---------|-------------|------------|-------|--------|-----------------------|
| IADLE | IIIuicators | calculateu | Daseu | OH UR | E EXDELITIELLAL GALA. |

| Dosage (w) (%) | 28-day UCS (kPa) | Strength gain (<i>SG(w</i>)) (kPa) | Performance-cost ratio (<i>PCR(w)</i>) (kPa/%) | Marginal strength gain (<i>MG</i> (w _i)) (kPa/%) |
|----------------|------------------|---|--|---|
| 5 | 267.2 | 183.5 | 36.7 | 36.7 |
| 10 | 326.9 | 243.2 | 24.32 | 11.94 |
| 15 | 378.1 | 294.4 | 19.63 | 10.24 |
| 20 | 357.6 | 273.9 | 13.7 | -4.1 |
| 25 | 364.6 | 280.9 | 11.24 | 1.4 |

UCS data used for calculations is from Figure 9.

optimal solution. Furthermore, its Performance-Cost Ratio (PCR) of 19.63 kPa/% is significantly higher than that of the 20% and 25% dosages, indicating superior overall efficiency.

The most decisive evidence is provided by the Marginal Strength Gain (MG) analysis. The MG remains strongly positive for the interval increasing to 15% (10.24 kPa/%). However, for the interval from 15% to 20%, the MG becomes negative (–4.10 kPa/%). This critical shift signifies that increasing the dosage beyond 15% is not only less efficient but is technically detrimental, causing a reduction in the soil's ultimate strength. This phenomenon confirms that 15% is the physical limit for effective strength enhancement. Therefore, the 15% dosage is robustly identified as the optimum, as it uniquely satisfies the peak performance criteria, exhibits the highest economic efficiency among feasible options, and represents the point of maximum effective treatment before the onset of negative returns.

4 Discussion on the mechanisms of soil stabilization

The stabilization of expansive soil by the combined use of ultrafine high-reactivity fly ash (UHFA) and calcium carbide slag (CCS) is governed by the coupling of three processes: alkaline activation and subsequent pozzolanic reactions, cation-exchange-driven double-layer compression, and microstructural densification through gel bridging and physical filling (as shown in Figure 11). The optimal proportion UHFA:CCS = 7:3 and the optimal dosage window of 15%–20% identified in the macroscopic tests can be rationalized by the balance among these mechanisms, which together transform a swelling-prone, fabric-sensitive clayey matrix into a cohesive, low-deformability skeleton. This transformation of a weak soil into a robust engineering composite is a central goal in geotechnical engineering, pursued through various chemical stabilization methods, as investigated here, and other approaches such as mechanical reinforcement (Ezazi et al., 2024).

The initiation of chemical stabilization relies on the alkaline environment supplied by CCS, a principle well-established for calcium-based additives like lime and cement (Hashemi et al., 2023). Calcium hydroxide from CCS dissolves in pore water, releasing Ca²⁺ and OH⁻ and elevating the system pH (Equation 4). This high-pH environment is crucial for activating pozzolanic

materials, a mechanism confirmed in early studies combining calcium carbide residue with fly ash (Horpibulsuk et al., 2012). Under high pH, the amorphous silica and alumina phases in UHFA depolymerize and dissolve, providing reactive silicate and aluminate species that participate in secondary hydration with Ca²⁺ to form calcium silicate hydrate (C-S-H) and calcium aluminate hydrate (C-A-H) (Equations 5 and 6). These nano-to micro-scale hydrates nucleate on particle surfaces, progressively establishing a continuous cemented network that explains the observed increases in unconfined compressive strength (UCS). The formation of this secondary C-S-H gel is also the primary mechanism when combining other pozzolans (like nano-silica) with lime, resulting in significant strength gains (Karimiazar et al., 2023).

$$Ca(OH)_2 \to Ca^{2+} + 2OH^-$$
 (4)

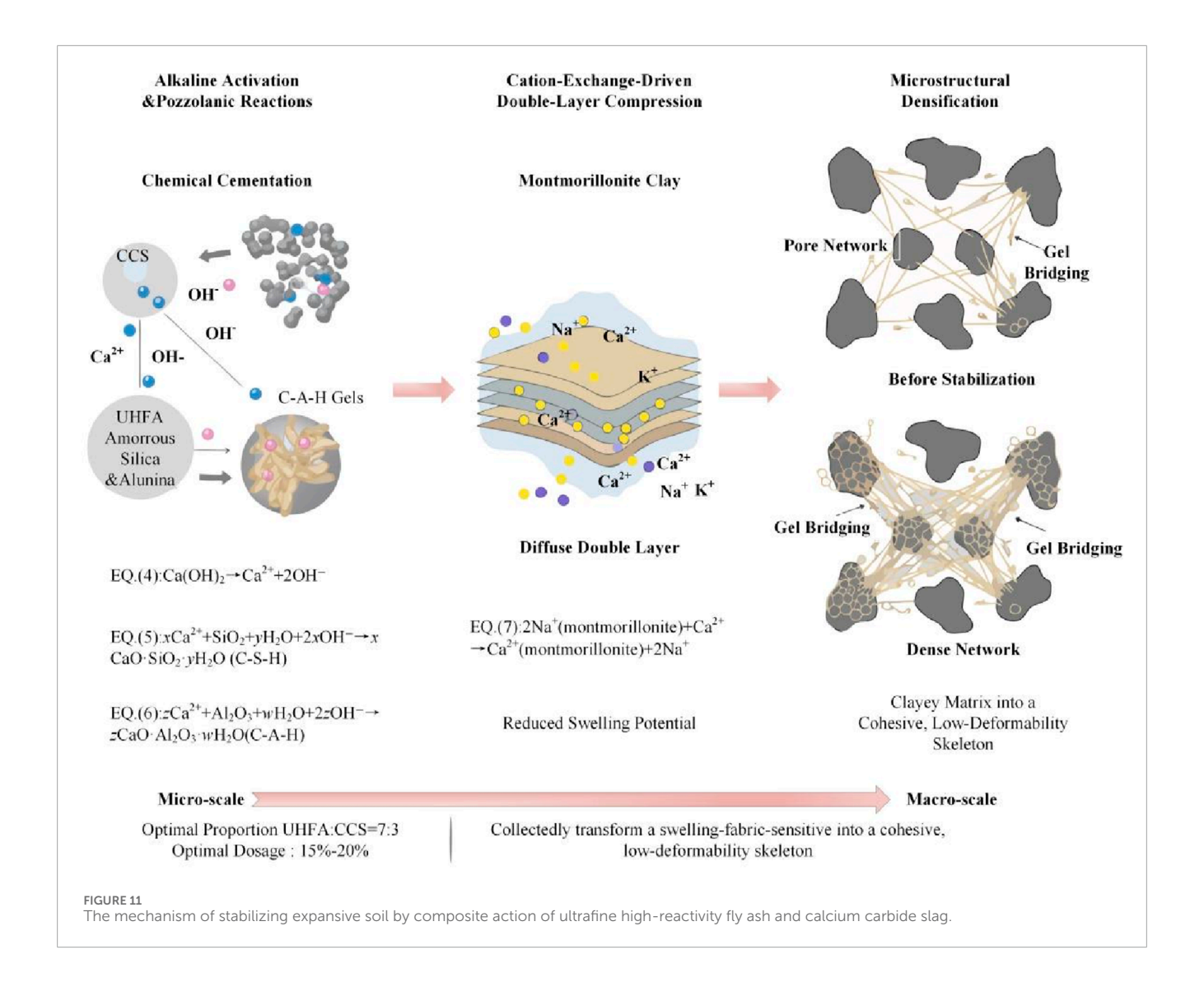
$$xCa^{2+} + SiO_2 + yH_2O + 2xOH^- \rightarrow xCaO \cdot SiO_2 \cdot yH_2O (C - S - H)$$
(5)

$$zCa^{2+} + Al_2O_3 + wH_2O + 2zOH^- \rightarrow zCaO \cdot Al_2O_3 \cdot wH_2O(C - A - H)$$
 (6)

A second, equally important pathway is the reduction of swelling potential through cation exchange. Expansive clays contain interlayer and diffuse-double-layer monovalent cations such as Na⁺ and K⁺, which have high hydration energies. Calcium ions released from CCS displace these monovalent cations, yielding Ca-saturated clay with a lower hydration tendency and a thinner diffuse double layer (Equation 7). This exchange reduces interparticle repulsion and facilitates flocculation, thereby suppressing macroscopic free swell. The monotonic decrease of the 28-day free swelling rate directly reflects this ion-exchange-driven double-layer compression acting in concert with gel formation.

$$2\text{Na}^+$$
(montmorillonite) + Ca^{2+} \rightarrow Ca^{2+} (montmorillonite) + 2Na^+

These chemical interpretations are directly substantiated by mineralogical analysis. Figure 12a presents the X-ray diffraction (XRD) pattern of the untreated expansive soil, where the primary crystalline phases are identified as common soil minerals, including Quartz and Illite. As expected, no peaks corresponding to cementitious hydration products are present. In stark contrast,



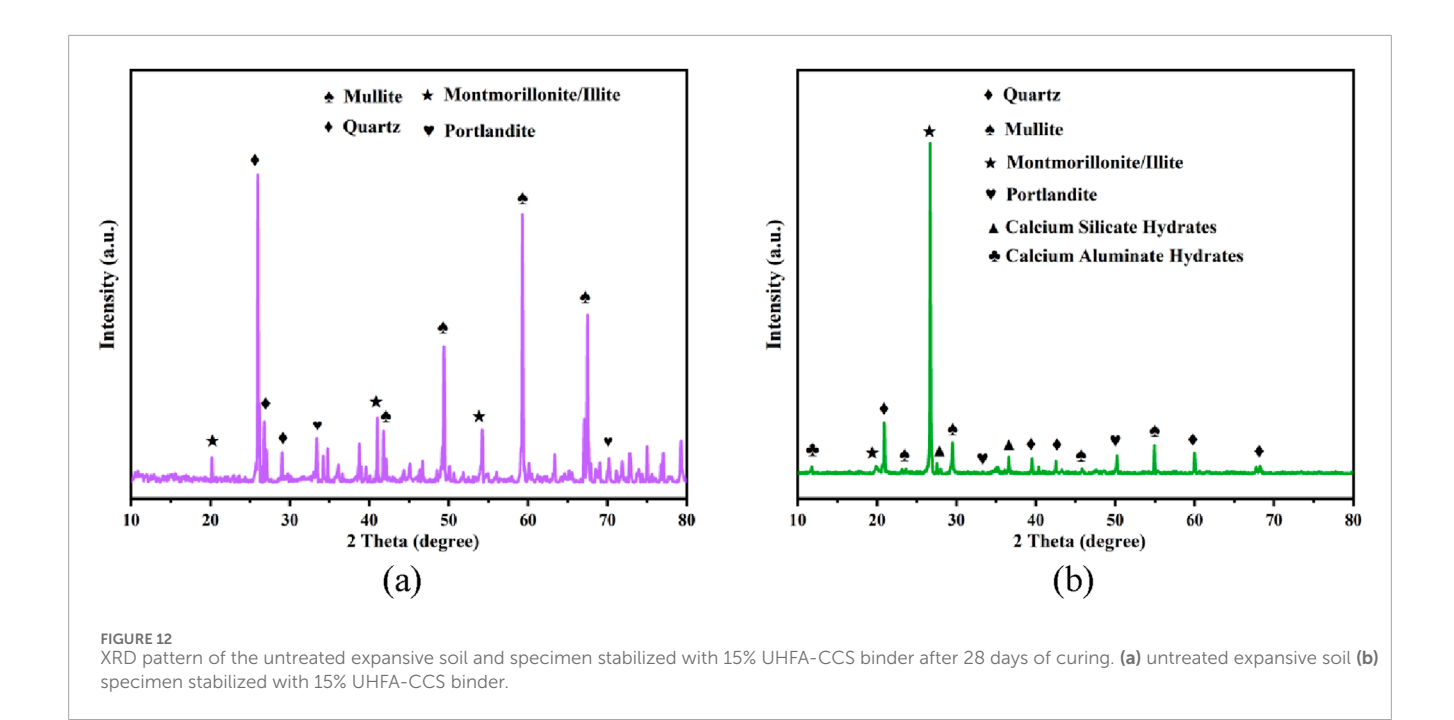
the XRD pattern of the soil stabilized with a 15% UHFA-CCS binder (cured for 28 days), shown in Figure 12b, reveals the formation of new crystalline and semi-crystalline phases. While the characteristic peaks of the original soil minerals (e.g., Quartz, Illite/Montmorillonite) persist, distinct new peaks identified as Calcium Silicate Hydrates (C-S-H) and Calcium Aluminate Hydrates (C-A-H) have appeared. The emergence of these new C-S-H and C-A-H peaks provides definitive proof of the pozzolanic reactions described in Equations 5 and 6, confirming that these new binding gels are the fundamental source of the observed strength gain.

Scanning electron microscopy (SEM) provides visual confirmation of the microstructural changes inferred from the chemical and mineralogical data. As shown in Figure 10, at a low dosage, only sparse hydrates bridge isolated contacts. At the 15% optimal dosage, C-S-H and C-A-H appear as an interconnected network that uniformly fills voids, producing a dense skeleton. This fabric explains the peak 28-day UCS of 378.1 kPa. This process of microstructural densification through gel formation is a common feature reported in soils stabilized with other synergistic binder systems, such as those using cement kiln dust

(Sharifi Teshnizi et al., 2024) or nano-additives combined with cement (Karimiazar et al., 2022). At 25% dosage, hydrate abundance increases but becomes locally agglomerated. Such heterogeneity accounts for the diminishing late-age strength gains, a finding consistent with studies on other blended systems where an excess of additives can reduce strength (Mirzababaei et al., 2021).

The emergence of an optimal binder dosage near 15% can be interpreted through reaction efficiency and percolation of the gel network. At approximately 15%, the supply of Ca²⁺ and OH⁻ from CCS is well matched to the reactive silica and alumina supplied by UHFA. This concept of an optimal content aligns with the findings of Horpibulsuk, Phetchuay and Chinkulkijniwat (Horpibulsuk et al., 2012), who identified "active" and "inert" zones of improvement. Beyond 20%, however, reaction-diffusion limitations and local agglomeration reduce efficiency. Early hydrates may encapsulate unreacted UHFA particles ("gel blocking"), limiting further dissolution. These factors rationalize the observed inverted-U relationship between dosage and 28-day UCS.

From an engineering standpoint, these mechanisms explain why the 15%–20% dosage range at the 7:3 proportion best reconciles performance and economy. At this level, cation exchange is



sufficient to suppress swelling into the non-expansive range by 28 days, while the hydrate network has percolated and continues to mature, delivering high UCS without necessitating excessive binder consumption or inducing microstructural heterogeneity. The formation of a continuous and stable hydrate skeleton, as proven by XRD and observed *via* SEM, is fundamental to resisting degradation and ensuring the longevity of the stabilized soil.

5 Summary and conclusion

This study systematically investigated the synergistic use of ultrafine high-reactivity fly ash (UHFA) and calcium carbide slag (CCS) to stabilize expansive soil, evaluating the engineering performance and underlying mechanisms through a comprehensive laboratory testing program. The influence of the binder's mix proportion and total dosage was analyzed to identify an optimal formulation for practical application. Based on the experimental results, the following key conclusions can be drawn.

- 1. The optimal mass ratio of UHFA to CCS was determined to be 7:3. This specific proportion achieves a superior balance between short-term workability and long-term performance, effectively suppressing the soil's swelling potential while facilitating the highest 28-day unconfined compressive strength (UCS) compared to other ratios. Ratios with higher UHFA content showed accelerated early strength gain but were ultimately limited by the insufficient alkaline activation from CCS for sustained pozzolanic reactions.
- 2. An optimal total binder dosage of 15% by dry soil mass is recommended for achieving maximum mechanical performance and economic efficiency. While dosages in the 15%-20% range effectively mitigate swelling and enhance

- strength, the 15% dosage yielded the peak 28-day UCS of 378.1 kPa. A marginal benefit analysis confirmed that dosages beyond 15% result in diminishing returns and can even be detrimental to ultimate strength, making the 15% dosage the most technically and economically sound option.
- 3. The optimized UHFA-CCS binder system significantly improves the engineering properties of expansive soil. At the optimal dosage of 15%, the 28-day free swelling rate was reduced to 27.4%, successfully reclassifying the material from expansive to non-expansive based on standard engineering criteria. Concurrently, the 28-day UCS reached 378.1 kPa, an approximate 4.5-fold increase over the untreated soil (83.7 kPa), demonstrating a profound enhancement in bearing capacity.
- 4. The stabilization is governed by a dual chemical and microstructural mechanism. The high alkalinity of CCS activates the pozzolanic reactivity of UHFA, leading to the formation of calcium silicate hydrate (C-S-H) and calcium aluminate hydrate (C-A-H) gels. These hydration products fill voids and bind soil particles into a dense, rigid skeleton, as confirmed by SEM observations. Simultaneously, Ca²⁺ ions released from CCS facilitate cation exchange, which compresses the diffuse double layer of clay particles and reduces their affinity for water, thus effectively controlling swelling.

While the proposed optimal mixture demonstrates significant short-term improvements, future research should focus on its long-term performance and durability under complex environmental conditions. Furthermore, direct shear strength tests (e.g., triaxial or direct shear) are recommended to quantify the cohesion and friction angle parameters needed for detailed engineering design and to validate the findings of this study for practical implementation.

Data availability statement

The original contributions presented in the study are included in the article/supplementary material, further inquiries can be directed to the corresponding author.

Author contributions

XQ: Formal Analysis, Methodology, Resources, Writing – original draft, Writing – review and editing. ZL: Data curation, Formal Analysis, Investigation, Writing – original draft. JZ: Investigation, Project administration, Resources, Writing – original draft, Writing – review and editing. WL: Conceptualization, Data curation, Formal Analysis, Funding acquisition, Investigation, Project administration, Visualization, Writing – original draft, Writing – review and editing.

Funding

The author(s) declare that financial support was received for the research and/or publication of this article. This work was supported by General Project of Xizang Natural Science Foundation (XZ202501ZR0114), Science and Technology Program of Jiangsu Provincial Department of Housing and Urban-Rural Development (2024ZD052), Jiangsu Province Industry University Research Project (FZ20241807), Xizang Civil water Conservancy and electric power Engineering Technology Research center open project (XZA202405CHP2008B).

References

Abdila, S. R., Abdullah, M. M. A. B., Ahmad, R., Burduhos Nergis, D. D., Rahim, S. Z. A., Omar, M. F., et al. (2022). Potential of soil stabilization using ground granulated blast furnace slag (GGBFS) and fly ash *via* geopolymerization method: a review. *Materials* 15 (1), 375. doi:10.3390/ma15010375

Akmalaiuly, K., Berdikul, N., Pundienė, I., and Pranckevičienė, J. (2023). The effect of mechanical activation of fly ash on cement-based materials hydration and hardened state properties. *Materials* 16 (8), 2959. doi:10.3390/ma16082959

Almuaythir, S., Zaini, M. S. I., Hasan, M., and Hoque, M. I. (2024). Sustainable soil stabilization using industrial waste ash: enhancing expansive clay properties. *Heliyon* 10 (20). doi:10.1016/j.heliyon.2024.e39124

American Coal Ash Association (2003). Fly Ash Facts for Highway Engineers. American coal ash Association. FHWA-IF-03-019, 18–19.

Barman, D., and Dash, S. K. (2022). Stabilization of expansive soils using chemical additives: a review. *J. Rock Mech. Geotechnical Eng.* 14 (4), 1319–1342. doi:10.1016/j.jrmge.2022.02.011

Biswas, N., Puppala, A. J., and Chakraborty, S. (2024). Experimental studies and sustainability assessments of quarry dust for chemical treatment of expansive soils. *Geotechnical Test. J.* 47 (1), 140–156. doi:10.1520/gtj20220243

Cai, M., Zhu, H., Wan, Y., Zhu, H., Rabczuk, T., and Zhuang, X. (2024). Using ultrafine fly ash to achieve low-carbon, high strength and high toughness engineered cementitious composites LC-HSTC. Case Stud. Constr. Mater. 20, e03259. doi:10.1016/j.cscm.2024.e03259

Chen, Y., Wang, H., Liu, S., Bao, W., Wang, F., and Li, B. Q. (2025). A method for simulating rock with inherent microcracks and calibrate its microscopic parameters. *Rock Mech. Rock Eng.*, 58, 5633–5652. doi:10.1007/s00603-025-04422-x

Dai, Z., Huang, K., Chi, Z., and Chen, S. (2024). Model test study on the deformation and stability of rainfall-induced expansive soil slope with weak interlayer. *Bull. Eng. Geol. Environ.* 83 (3), 76. doi:10.1007/s10064-024-03576-2

Dang, L. C., Khabbaz, H., and Ni, B. J. (2021). Improving engineering characteristics of expansive soils using industry waste as a sustainable application

Conflict of interest

Authors XQ and ZL were employed by PowerChina Chengdu Engineering Corporation Limited. Author WL was employed by Jiangsu Hanjian Group Co., Ltd.

The remaining author declares that the research was conducted in the absence of any commercial or financial relationships that could be construed as a potential conflict of interest.

Generative AI statement

The author(s) declare that no Generative AI was used in the creation of this manuscript.

Any alternative text (alt text) provided alongside figures in this article has been generated by Frontiers with the support of artificial intelligence and reasonable efforts have been made to ensure accuracy, including review by the authors wherever possible. If you identify any issues, please contact us.

Publisher's note

All claims expressed in this article are solely those of the authors and do not necessarily represent those of their affiliated organizations, or those of the publisher, the editors and the reviewers. Any product that may be evaluated in this article, or claim that may be made by its manufacturer, is not guaranteed or endorsed by the publisher.

for reuse of bagasse ash. *Transp. Geotech.* 31, 100637. doi:10.1016/j.trgeo. 2021.100637

Ezazi, M., Hossaini, M. F., Sheikhmali, R., Khosrotash, M., Sharifi Teshnizi, E., and O'Kelly, B. C. (2024). Assessment of steel-fiber-reinforced segmental lining of chamshir water conveyance tunnel, Iran: integrating laboratory experiments, field observations, and numerical analysis. *Case Stud. Constr. Mater.* 20, e03144. doi:10.1016/j.cscm.2024.e03144

Fu, H., Tian, J., Chin, C. L., Liu, H., Yuan, J., Tang, S., et al. (2025). Axial compression behavior of GFRP-steel composite tube confined seawater sea-sand concrete intermediate long columns. *Eng. Struct.* 333: 120157, doi:10.1016/j.engstruct.2025.120157

Hashemi, H., Yazdi, A., and Sharifi Teshnizi, E. (2023). Improvement of collapsing problematic soils on the sabzevar-mashhad railway route (northeast of Iran) using traditional additives. *Nexo Rev. Cientifica* 36 (03), 383–403. doi:10.5377/nexo.v36i03.16461

Horpibulsuk, S., Phetchuay, C., and Chinkulkijniwat, A. (2012). Soil stabilization by calcium carbide residue and fly ash. *J. Mater. Civ. Eng.* 24 (2), 184–193. doi:10.1061/(asce)mt.1943-5533.0000370

Ikeagwuani, C. C., and Nwonu, D. C. (2019). Emerging trends in expansive soil stabilisation: a review. *J. Rock Mech. Geotechnical Eng.* 11 (2), 423–440. doi:10.1016/j.jrmge.2018.08.013

Jalal, F. E., Xu, Y., Iqbal, M., Jamhiri, B., and Javed, M. F. (2021). Predicting the compaction characteristics of expansive soils using two genetic programming-based algorithms. *Transp. Geotech.* 30, 100608. doi:10.1016/j.trgeo.2021.100608

Karami, H., Pooni, J., Robert, D., Costa, S., Li, J., and Setunge, S. (2021). Use of secondary additives in fly ash based soil stabilization for soft subgrades. *Transp. Geotech.* 29, 100585. doi:10.1016/j.trgeo.2021.100585

Karimiazar, J., Sharifi Teshnizi, E., Mirzababaei, M., Mahdad, M., and Arjmandzadeh, R. (2022). California bearing ratio of a reactive clay treated with nano-additives and cement. *J. Mater. Civ. Eng.* 34 (2), 04021431. doi:10.1061/(asce)mt.1943-5533.0004028

Karimiazar, J., Sharifi Teshnizi, E., O'Kelly, B. C., Sadeghi, S., Karimizad, N., Yazdi, A., et al. (2023). Effect of nano-silica on engineering properties of lime-treated marl soil. *Transp. Geotech.* 43, 101123. doi:10.1016/j.trgeo.2023.101123

- Li, Y., Li, J., Cui, J., Shan, Y., and Niu, Y. (2021). Experimental study on calcium carbide residue as a combined activator for coal gangue geopolymer and feasibility for soil stabilization. *Constr. Build. Mater.* 312, 125465. doi:10.1016/j.conbuildmat.2021.125465
- Liu, M., and Shu, S. (2025). Investigation of creep behavior and its effect on dilatancy of rockfill materials through large-scale triaxial testing. *J. Geotechnical Geoenvironmental Eng.* 151 (11), 04025132. doi:10.1061/jggefk.gteng-13311
- Lv, T., Zhang, J., Hou, D., Long, W.-J., and Dong, B. (2025). Mechanical-thermal activated dredged sludge as a supplementary cementitious material: microstructure reconstruction and pozzolanic activity enhancement. *Constr. Build. Mater.* 476, 141256. doi:10.1016/j.conbuildmat.2025.141256
- Ministry of Construction P.R.China (2019). GB/T 50123-2019 standard for soil test method. Beijing: China Planning Press.
- Mirzababaei, M., Karimiazar, J., Sharifi Teshnizi, E., Arjmandzadeh, R., and Bahmani, S. H. (2021). Effect of nano-additives on the strength and durability characteristics of marl. $\it Minerals$ 11 (10), 1119. doi:10.3390/min11101119
- Puppala, A. J. (2021). Performance evaluation of infrastructure on problematic expansive soils: characterization challenges, innovative stabilization designs, and monitoring methods. *J. Geotechnical Geoenvironmental Eng.* 147 (8), 04021053. doi:10.1061/(asce)gt.1943-5606.0002518
- Sharifi Teshnizi, E., O'Kelly, B. C., Karimiazar, J., Moosazadeh, S., Arjmandzadeh, R., and Pani, A. (2022). Effects of cement kiln dust on physicochemical and geomechanical properties of loess soil, Semnan province, Iran. *Arabian J. Geosciences* 15, 1482. doi:10.1007/s12517-022-10751-w
- Sharifi Teshnizi, E., Mirzababaei, M., Karimiazar, J., Arjmandzadeh, R., and Mahmoudpardabad, K. (2024). Gypsum and rice husk ash for sustainable stabilization of forest road subgrade. *Q. J. Eng. Geol. Hydrogeology* 57 (1), qjegh2023–008. doi:10.1144/qjegh2023-008
- Snellings, R., Kazemi-Kamyab, H., Nielsen, P., and Van den Abeele, L. (2021). Classification and milling increase fly ash pozzolanic reactivity. *Front. Built Environ.* 6, 670996. doi:10.3389/fbuil.2021.670996
- Sun, Y., Zhang, F., and Shu, S. (2025). Fabrication and interface shearing test of a meta-geocell. *Acta Geotech.*, 1–15. doi:10.1007/s11440-025-02668-x

- Teshnizi, E. S., Karimiazar, J., and Baldovino, J. A. (2023). Effect of acid and thermomechanical attacks on compressive strength of geopolymer mortar with different ecofriendly materials. *Sustainability* 15 (19), 14407. doi:10.3390/su151914407
- Tong, L., Fu, L., Wu, B., Xu, C., and Lim, C. W. (2025a). Packing fraction effect on dynamic creep deformation of granular materials. *Acta Geotech*. 20(5), 2135–2144. doi:10.1007/s11440-024-02459-w
- Tong, L., Fu, L., Wu, B., Xu, C., Lim, C. W., and Ding, H. (2025b). Particle shape effect on creep and fluidity of granular packing. *J. Eng. Mech.* 151(11): 04025067, doi:10.1061/jenmdt.emeng-8435
- Wang, J., and Dong, H. (2023). PVA fiber-reinforced ultrafine fly ash concrete: engineering properties, resistance to chloride ion penetration, and microstructure. *J. Build. Eng.* 66, 105858. doi:10.1016/j.jobe.2023.105858
- White, D., Harrington, D., Rupnow, T., and Ceylan, H. (2005). Fly ash soil stabilization for non-uniform subgrade soils (TR-461). Ames, IA: Iowa State University—Center for Transportation Research and Education.
- Yao, J., Cai, D., Su, K., and Yan, H. (2024). Nonlinear regression modeling of swelling characteristics in cracked expansive soil: integrating crack, moisture, density, and load effect. *Front. Mater.* 11, 1467134. doi:10.3389/fmats.2024.1467134
- Yu, Y., Su, J., and Wu, B. (2025). A hybrid Bayesian model updating and non-dominated sorting genetic algorithm framework for intelligent mix design of steel fiber reinforced concrete. *Eng. Appl. Artif. Intell.* 161, 112071. doi:10.1016/j.engappai.2025.112071
- Zada, U., Jamal, A., Iqbal, M., Eldin, S. M., Almoshaogeh, M., Bekkouche, S. R., et al. (2023). Recent advances in expansive soil stabilization using admixtures: current challenges and opportunities. *Case Stud. Constr. Mater.* 18, e01985. doi:10.1016/j.cscm.2023.e01985
- Zhang, C., Fu, J., Song, W., Du, C., and Fu, H. (2021). High-volume ultrafine fly ash-cement slurry mechanical properties and strength development model establishment. *Constr. Build. Mater.* 277, 122350. doi:10.1016/j.conbuildmat.2021.122350
- Zhang, F., Ji, W., Gao, Y., Leshchinsky, D., and Vahedifard, F. (2026). Thermal effects on the stability of geosynthetic reinforced soil walls. *J. Geotechnical Geoenvironmental Eng.*
- Zimar, Z., Robert, D., Sidiq, A., Zhou, A., Giustozzi, F., Setunge, S., et al. (2022). Waste-to-energy ash for treating highly expansive clays in road pavements. *J. Clean. Prod.* 374, 133854. doi:10.1016/j.jclepro.2022.133854